DOI: 10.1590/2317-4889201530124

ARTICLE

Late Pleistocene sea-level changes recorded in tidal and fluvial deposits from Itaubal Formation, onshore portion of the Foz do Amazonas Basin, Brazil

Mudanças no nível do mar durante o Pleistoceno Tardio registradas em depósitos fluviais e influenciados por maré da Formação Itaubal, porção onshore da Bacia da Foz do Amazonas, Brasil

Isaac Salém Alves Azevedo Bezerra[1]*, Afonso César Rodrigues Nogueira[1], José Tasso Felix Guimarães[1,2], Werner Truckenbrodt[1]

ABSTRACT: The Pleistocene deposits exposed in the Amapá Coastal Plain (onshore portion of the Foz do Amazonas Basin, northeastern South America) were previously interpreted as Miocene in age. In this work, they were named as "Itaubal Formation" and were included in the quaternary coastal history of Amazonia. The study, through facies and stratigraphic analyses in combination with optically stimulated luminescence (single and multiple aliquot regeneration), allowed interpreting this unit as Late Pleistocene tidal and fluvial deposits. The Itaubal Formation, which unconformably overlies strongly weathered basement rocks of the Guianas Shield, was subdivided into two progradational units, separated by an unconformity related to sea-level fall, here named as Lower and Upper Units. The Lower Unit yielded ages between 120,600 (± 12,000) and 70,850 (± 6,700) years BP and consists of subtidal flat, tide-influenced meandering stream and floodplain deposits, during highstand conditions. The Upper Unit spans between 69,150 (± 7,200) and 58,150 (± 6,800) years BP and is characterized by braided fluvial deposits incised in the Lower Unit, related to base-level fall; lowstand conditions remained until 23,500 (± 3,000) years BP. The studied region was likely exposed during the Last Glacial Maximum and then during Holocene, covered by tidal deposits influenced by the Amazon River.

KEYWORDS: Amazonia; Pleistocene; sea-level changes; coastal deposits; Itaubal Formation.

RESUMO: *Depósitos pleistocenos expostos na Planície Costeira do Amapá (porção onshore da Bacia da Foz do Amazonas, nordeste da América do Sul) foram anteriormente interpretados como de idade miocena. Neste trabalho, esses depósitos foram chamados de "Formação Itaubal" e incluídos na evolução costeira quaternária da Amazônia. O estudo, mediante o uso de análise de fácies e estratigrafia em combinação com luminescência opticamente estimulada (regeneração de alíquotas simples e múltiplas), permitiu posicionar essa unidade no Pleistoceno Tardio, interpretada como depósitos fluviais e influenciados por maré. A Formação Itaubal, que sobrepõe discordantemente rochas intensamente intemperizadas do embasamento do Escudo das Guianas, foi subdividida em Unidade Inferior e Superior, de caráter progradante, separadas por desconformidade relacionada à queda do nível do mar. A Unidade Inferior apresenta idades entre 120.600 (± 12.000) e 70.850 (± 6.700) anos AP e consiste de depósitos de submaré, canal fluvial meandrante influenciado por maré e depósitos de planície de inundação, depositados durante condições de nível de mar alto. A Unidade Superior apresenta idades entre 69.150 (± 7.200) e 58.150 (± 6.800) anos AP e é caracterizada por depósitos de canal entrelaçado, que retrabalham a Unidade Inferior, depositada em condições relacionadas à queda do nível de base. Condições de nível de mar baixo permaneceram até 23.500 (± 3.000) anos AP. A região estudada foi provavelmente exposta durante o Último Máximo Glacial e, posteriormente, durante o Holoceno, recoberta por depósitos influenciados por maré oriundos do Rio Amazonas.*

PALAVRAS-CHAVE: *Amazônia; Pleistoceno; mudanças no nível do mar; depósitos costeiros; Formação Itaubal.*

[1]Programa de Pós-Graduação em Geologia e Geoquímica, Universidade Federal do Pará – UFPA, Belém (PA), Brasil. *E-mail: isaac.bezerra@ig.ufpa.br; anogueira@ufpa.br; trucken@ufpa.br*

[2]Instituto Tecnológico Vale., Belém (PA), Brasil. *E-mail: tasso.guimaraes@vale.com*

*Corresponding author.

Manuscript ID: 30124. **Received:** 06/06/2014. **Approved:** 02/18/2015.

INTRODUCTION

The Cenozoic siliciclastics deposits exposed in the Amapá Coastal Plain (ACP) have traditionally been interpreted as alluvial fans, fluvial and lacustrine deposits representative of the Miocene Barreiras Formation, a characteristic unit mainly exposed along the northern and northeastern Brazilian coast, and sand and muddy terraces deposits formed by sediments derived from the Amazon River, during Holocene (Lima *et al*. 1974, 1991; Mendes 1994; Silveira 1998; IBGE 2003; CPRM 2004; Santos 2006; Guimarães *et al*. 2013a, 2013b). However, Souza (2010) suggests tidal influence in Miocene deposits and, based on low-resolution optically stimulated luminescence — OSL (multiple aliquot regeneration), indicates Late Pleistocene age for the older rocks.

In this work, we reviewed the older rocks using facies and stratigraphic analyses in combination with high-resolution OSL (single and multiple aliquot regeneration). Our data confirm the Late Pleistocene age and the influence of sea-level changes in these deposits, named here as "Itaubal Formation". Two progradational units can be differentiated: a Lower Unit, consisting of tide-influenced deposits, and an Upper Unit, comprising mainly fluvial sediments. Until now, the Pleistocene deposits have been described only in the coast of French Guiana (Coswine Formation; Boye and Cruys 1961) and Suriname (Coropina Formation; Roeleveld and Van Loon 1979; Krook 1979; Wong *et al*. 2009), 200 km to the north of the ACP. The Itaubal Formation can be correlated with Pós-Barreiras sediments, exposed in the Marajó Graben and Bragantina Platform, northern coast of Brazil; (Rossetti *et al*. 1989; Rossetti 2004; Rossetti and Valeriano 2007). Pleistocene deposits exposed in the ACP, onshore portion of the Foz do Amazonas Basin, northeastern South America, are included now in the Quaternary coastal history of Amazonia.

REGIONAL SETTING

The siliciclastics Pleistocene deposits of the eastern portion of the ACP overlie the Archean to Mesoproterozoic basement of the Guianas Shield, composed of crystalline and metasedimentary rocks (Fig. 1; Lima *et al.* 1974, 1991; Souza 2010).

The study area is located in the onshore portion of the Foz do Amazonas Basin, comprising the Amapá Platform (Fig. 1A), while the offshore portion of this region is represented in the Amazon Fan that also includes the Marajó Basin (Grossmann 2002; Soares Júnior *et al*. 2008). The northwestern and southeastern limits of the basin are the Demerara Plateau and the Santana Island of the Pará-Maranhão Basin, respectively (Brandão and Feijó 1994).

The Foz do Amazonas Basin is linked to the Marajó Graben System evolution related to several episodes of extensional tectonics succeeded by Gondwana break up and opening of the Equatorial Atlantic from the Triassic to the Cretaceous (Galvão 1991; Rodarte and Brandão 1988; Soares Júnior *et al.* 2008). The Neogene-Quaternary sedimentation in the Foz do Amazonas basin was influenced by climatic and global sea-level changes, associated with the establishment of the paleo-Amazon River during the Late Miocene (Miller *et al*. 1987; Haq *et al*. 1988; Lopez 2001; Uba *et al*. 2007; Garzione *et al*. 2008; Souza 2010). The onset of the Amazon Fan was characterized by deposition of the Tucunaré, Pirarucu and Orange Formations constituting the Pará Group (Brandão and Feijó 1994; Figueiredo *et al*. 2009). During the Pleistocene to Holocene, sea-level changes caused subaerial exposure succeeded by flooding of the Amapá Platform (Lopez 2001; Souza 2010).

METHODS

The deposits of the Itaubal Formation were studied on the roadcuts of BR-156 highway, near the town of Tartarugalzinho, State of Amapá, Brazil, about 100 km inland from the coastline and 15 to 20 m above sea-level (Fig. 1B). There, they form a 10 m thick interval of sand and clays with subordinate gravels.

Stratigraphic logs and panoramic sections were described and photographed, and paleocurrent data were measured. The obtained information was used in making facies analysis and stratigraphic correlation (Walker 1992; Miall 1991, 1994). Grain size analyses using classic sieving methods of Folk (1974) completed the facies data.

Ten samples of medium to coarse sand were collected for high-resolution OSL dating (single and multiple aliquot regeneration — OSL/SAR-MAR), following the procedures of Murray and Wintle (2000). The samples were analyzed in the Faculdade de Tecnologia do Estado de São Paulo (FATEC) with a Photomultiplicator Thorn EMI Electron Tubes, Type 9235QA, for accumulated doses and with a Canberra Inspector Portable Spectroscopy Workstation (NaI - Tl) for annual doses. More details about the application of OSL/SAR-MAR protocols in Pleistocene deposits of the northern Brazilian coast can be found in Tatumi *et al.* (2008) and Rossetti *et al.* (2013).

RESULTS

Optically stimulated luminescence dating

Considering the OSL/SAR dating, the sediment samples in log TR2 yielded ages of 120,600 (± 12,000), 99,800 (± 12,200) and 70,850 (± 6,700) years BP, while ages of 100,000 (± 11,500), 96,800 (± 8,250) and 75,300 (± 8,500) years BP were obtained in log TR1, TR4 and TR5, respectively (Fig. 2; Tab. 1). The youngest ages were detected in log TR5, with 69,150 (± 7,200) years BP, and in log TR3, with 58,150 (± 6,800) years BP (Fig. 2; Tab. 1).

Considering the OSL/MAR dating, the sediment samples in log TR2 yielded an age of 78,000 (± 12,000) years BP. The youngest age was detected in log TR6, with 23,000 (± 3,000) years BP (Fig. 2; Tab. 1).

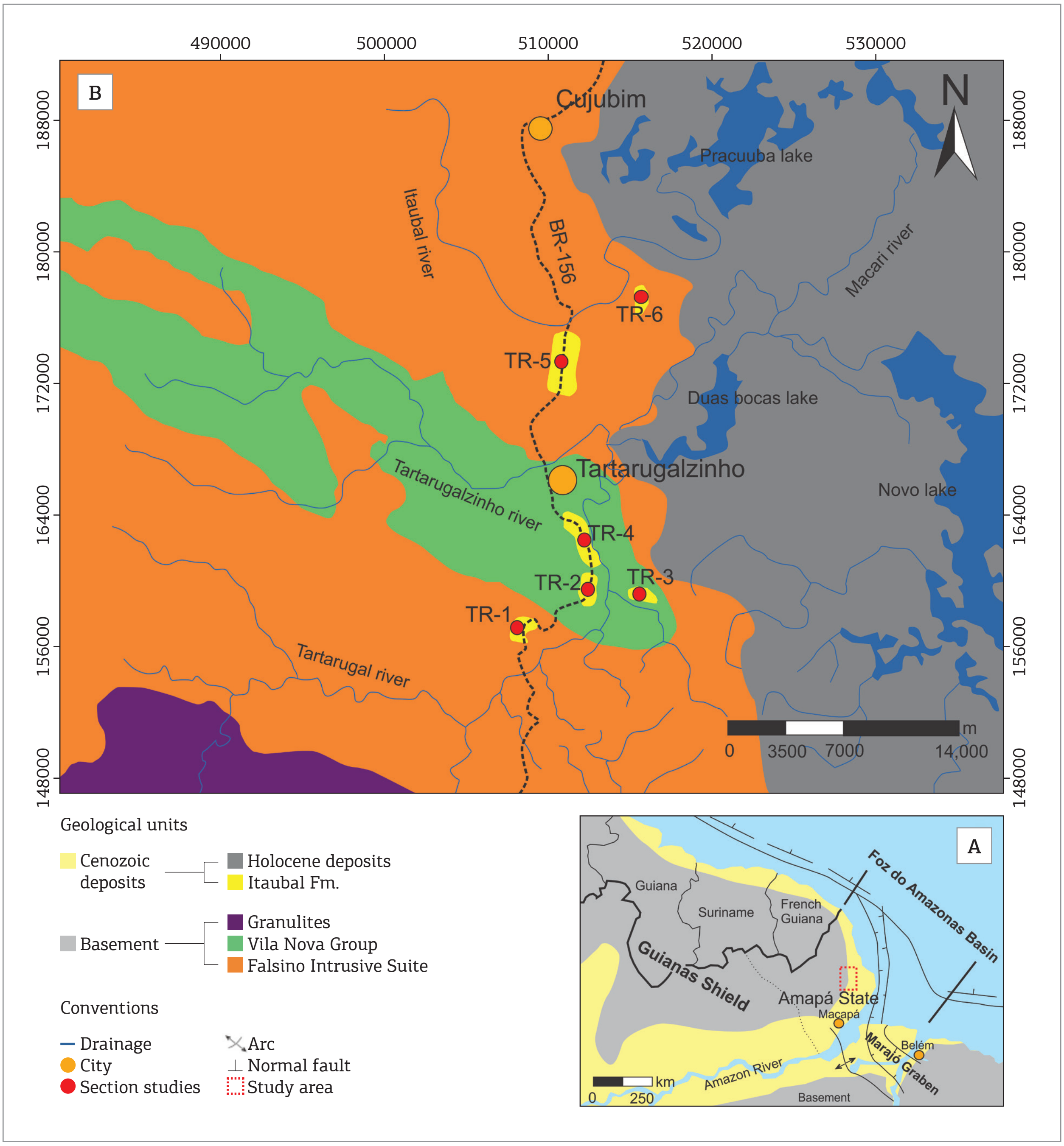

Figure 1. (A) Geological settings of Norteastern South America and location of study area. (B) Geological map of the onshore portion of the Foz do Amazonas Basin, with the location of the studied sections of the Itaubal Formation (Souza 2010).

Facies analysis

The succession of the Itaubal Formation consists predominantly of very fine to coarse sands and clay, locally gravel (with rare boulders), organized in centimeter-scale coarsening-upward cycles. This formation overlying an unconformity developed on strongly weathered basement crystalline rocks. Pleistocene deposits are also weathered and, many times, their distinction of the weathered basement rocks is difficult. The Itaubal Formation was subdivided into two units, separated by an unconformity, and comprises four facies associations (FA). The Lower Unit is represented by subtidal flat deposits (FA1), tide-influenced meandering- stream deposits (FA2) and floodplain deposits, while the Upper Unit is characterized by braided stream deposits (FA3) (Fig. 2; Tab. 2). In the following paragraphs, facies associations are discussed. For a more detailed description of facies, see Tab. 2.

Lower unit

The 6-m-thick succession of the Lower Unit is mainly composed of granules with boulders (> 25.6 cm), very fine sand and silt, showing brownish to reddish and subordinately whitish to yellowish colors, related to strong weathering and ferruginization. The sandy deposits form tabular beds up to

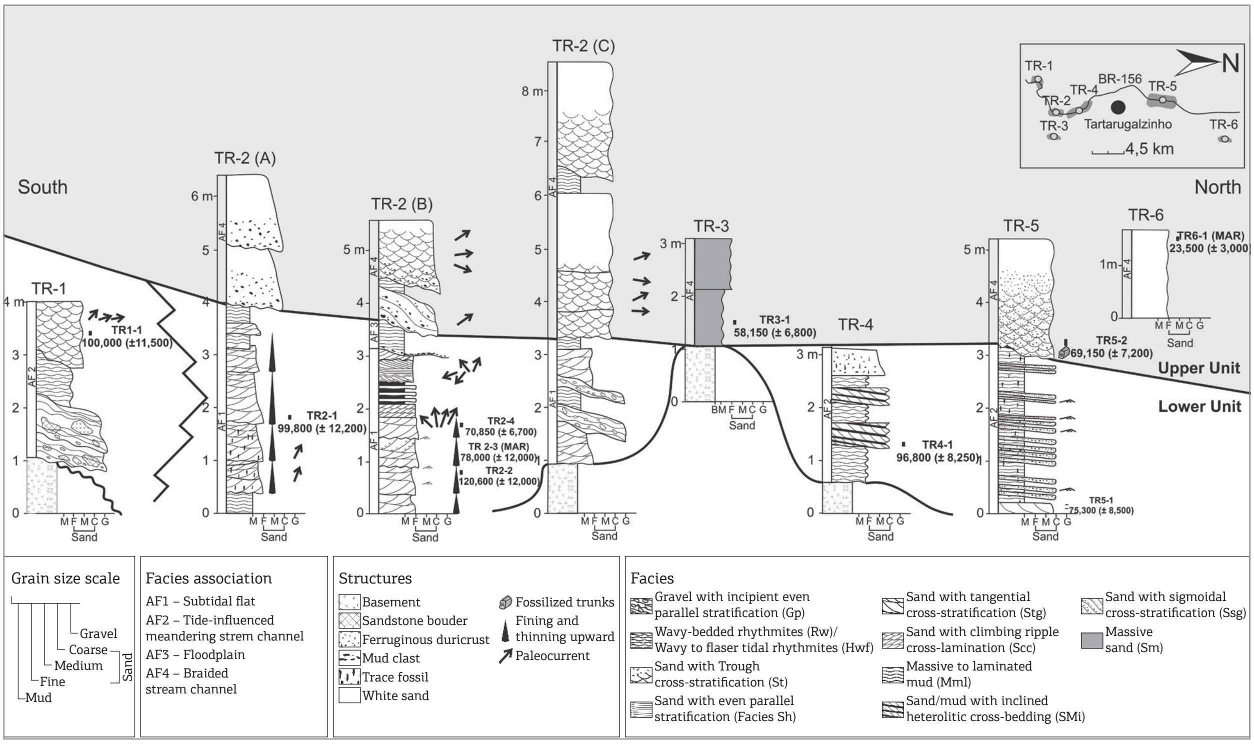

Figure 2. Stratigraphic logs of the Itaubal Formation.

Table 1. Radioactive data, annual dose values and OSL/SAR-MAR ages of the sediment samples.

Sample name	Protocol	Th (ppm)	U (ppm)	K (%)	Annual dose (µG/yr)	Accumulated dose	Mean Age (yr BP)
TR6-1	MAR	6,234 ± 0,224	1,852 ± 0,161	0,520 ± 0,075	1.730 ± 130	40,78	23,500 ± 3,000
TR5-2	SAR	16,514 ± 0,595	4,578 ± 0,280	0,242 ± 0,035	2830 ± 155	195,4	69,150 ± 7,200
TR5-1	SAR	4,892 ± 0,176	1,693 ± 0,038	0,466 ± 0,068	1470 ± 90	110,8	75,300 ± 8,500
TR4-1	SAR	9,523 ± 0,343	2,507 ± 0,080	0,070 ± 0,010	1610 ± 60	156,1	96,800 ± 8,250
TR3-1	SAR	13,500 ± 0,486	4,666 ± 0,030	1,375 ± 0,199	3690 ± 250	214,6	58,150 ± 6,800
TR2-4	SAR	16,706 ± 0,601	4,678 ± 0,154	0,290 ± 0,042	2880 ± 130	204,2	70,850 ± 6,700
TR2-3	MAR	8,221 ± 0,296	1,719 ± 0,421	0,154 ± 0,022	1470 ± 150	114,50	78,000 ± 12,000
TR2-2	SAR	7,597 ± 0,273	2,421 ± 0,140	0,128 ± 0,019	1500 ± 75	180,4	120,600 ± 12,000
TR2-1	SAR	6,444 ± 0,232	2,615 ± 0,140	0,545 ± 0,079	1890 ± 135	188,0	99,800 ± 12,200
TR1-1	SAR	9,025 ± 0,325	2,902 ± 0,282	0,083 ± 0,012	1680 ± 110	167,9	100,000 ± 11,500

Table 2. Summary of facies descriptions and sedimentary processes in the Itaubal Formation.

Facies	Description	Process	FA
Upper Unit			
Coarse sand with trough cross-stratification (Facies St)	Medium to coarse sands with trough cross-stratification with set thickness up to 2.5 m; quartz and brownish, deformed mud granules scattered at the base. Grains are poorly- to moderately sorted.	Migration of 3D bedforms with sinuous crests under lower flow regime. Reworking of mud beds in hydroplastic condition.	Braided stream channel (FA4)
Sand with tabular cross-stratification (Facies Sp)	Brownish, medium sands with tabular cross-stratification. Beds are lenticular, up to 1 m thick, and interbedded with Facies St.	Migration of 2D bedforms with straight crests under lower flow regime.	
Sand with sigmoidal cross-stratification (Facies Ssg)	Brownish medium sands with sigmoidal cross-stratification with sets covered by clay laminae, and interbedded with Facies Mml of the FA3.The grains are poorly-sorted, displaying positive asymmetry and kurtosis with leptokurtic distribution.	Bedform migration under unidirectional and lower flow regime, with rapid deceleration when it reaches a floodplain lake or pound. Clay laminae can also be formed by gradual deposition in this process.	
Massive muds (Facies Mm)	Whitish to reddish, centimetric beds of massive clay with lenticular geometry, filling curved base of beds.	Deposition of mud under slack water conditions	
Lower Unit			
Intraformational massive mud clast (Gi)	Yellowish to reddish, massive laminae of gravels, formed by intraformational mud pebbles and cobbles.	Reworking of laminated mud beds by energetic flood fluvial process.	Floodplain (FA3)
Massive to laminated mud (Facies Mml)	Reddish-whitish, laminated mud beds of up to 50 cm, interbedded with sigmoidal cross-stratification that, in general, fills channelized bedforms.	Alternation between traction and mainly gravitational settling from suspension.	
Gravel with incipient, even parallel stratification (Facies Gp)	Brownish to whitish, channelized beds with gravel of lag deposits from basement rocks and ferruginous sandstone boulders (up to 82 cm).	High to moderate flows generating scours in talweg portions of channels. Lateral migration produces intense reworking of ferruginized ancient siliciclastics deposits and basement rocks.	Tide-influenced meandering stream channel(FA2)
Medium- to coarse-grained sands with trough cross-stratification (Facies St)	Whitish coarse-sand beds with trough cross-stratification (sets up to 35 cm thick). Scattered quartz pebbles in the base of sets. The grains moderately-sorted.	Migration of 3D bedforms with sinuous crests in longitudinal bedforms, under high to moderate flow regime.	
Medium-grained sand with tangential cross-stratification (Facies Stg)	Reddish medium sands forming tabular sets of tabular to tangential planar cross-bedding. They are truncated by sets of facies Sth.	Migration of 2D bedforms on the channel complex bar, under moderate flow regime.	
Hetherolitic cross-bedding sets with alternating sand and mud laminae (Facies SMi)	Dark brown to whitish, inclined medium to coarse sand beds alternating with mud laminae. They can be interbedded with Facies Mml. The grains are moderately-to poorly-sorted. The upper portion of the strata is marked by ripple marks.	Lateral accretion in concave marginal portions with sand and mud deposited during moderate- and low-energy flows, respectively, of large to medium-scale point bars. Small-scale bedforms can also migrate onto these bedforms.	
Wavy-bedded rhythmites (Facies Rw)	Centimetric to metric yellowish to brownish wavy mud laminae alternated with ripple-bedded fine sand layers that can be interbedded with Facies SMi.	Alternating periods of mud and sand deposition from suspension and bedload transport, respectively.	
Fine-grained sands with trough cross-stratification (Facies St)	Reddish, fine to medium sand with trough cross-stratification with sets up 30 cm thick. Bedding planes and foresets are covered by clay laminae. Intraformational granules with rounded to tabular clay granules occur scattered along the bottom set.	Migration of 3D bedforms with sinuous crest under high to moderate energy and tidal influence, with alternation between traction and suspension processes. Bedform migration during flood tidal current, reworking clay laminae deposited during slack-water conditions.	Subtidal flat (FA1)
Fine-grained sand with tabular cross-stratification (Facies Sp)	Reddish, fine to medium sand beds with thickness varying from 20 to 50 cm, with tabular cross-stratification, and cyclic variations of foreset thickness. Bedding planes and foresets, are locally covered by clay laminae.	Migration of 2D subaqueous bedforms with straight crests. This process alternates with slack-water conditions forming mud drapes on the foresets. Variations in the foreset thickness are related with neap-spring cycles.	
Fine-grained sand with tangential cross-stratification (Facies Stg)	Reddish fine to medium sands with tangential to quasi-tabular planar cross-stratification interbedded with Facies Sth. Mud drapes occur in the foresets and bedding planes.	Migration of 2D bedforms in subtidal conditions, with alternations between traction and suspension processes.	
Sand with climbing ripple cross-lamination (Facies Scc)	Reddish-pinkish, centimetric, fine to medium sand with subcritical climbing cross-lamination. Locally slight reworking of the top set of the Facies St and Sp.	Migration of 2D ripples with straight crests, with predominance of traction in detriment of settling from suspension processes. Oscillations of dominant energy flow can be indicated reworking of Facies St and Sp.	
Bioturbated sand (Facies Sb)	Sand beds with intense bioturbation, interbedded with Facies Sth and St.	Intense mixture of fine-grained sand sediments by bioturbation.	
Sand with sigmoidal cross-stratification (Facies Ssg)	Sands with sigmoidal cross-stratification, about 15 cm thick. Reworked mud clasts can also be observed in the foresets.	Bedform migration with rapid decceleration of the water flow. Dominant current reworks clay laminae deposited during slack water.	
Sand with even parallel stratification (Facies Sh)	Centimetric to metric, coarse to medium sand with planar stratification, locally bioturbated.	Plane-bed flow under upper flow regime. After this conditions, some organism can be mixture this sediments.	
Wavy to flaser tidal rhythmites (Facies Hwf)	Centimetric to metric, yellowish to brownish beds with alternation between massive or laminated sands and mud forming wavy to flaser structures.	Alternation between traction currents that deposited laminated sands (2-D ripples) and slack-water conditions, with deposition of massive mud, during tidal currents and slack-water, respectively.	
Massive mud (Facies Mm)	Massive mud beds.	Deposition of mud under slack-water conditions.	

FA: facies association.

2.5-m thick, extending laterally hundreds of meters and locally show channelized geometry (Fig. 3). Bedforms and foresets of cross-bedding sets are commonly covered by mud drapes. Paleocurrent trends of cross-bedding are towards NW, N and NE, while a NE-SW bidirectional pattern was obtained from herringbone-cross stratified sands.

Subtidal flat (FA1)

This facies association forms the lower portion of the Lower Unit, which onlaps the weathered rocks of the basement (Figs. 4A and 4B) and consists of sandy and muddy deposits. The sandy deposits are generally fine-grained and display tabular cross-stratification (Facies Sp), climbing ripple cross-lamination (Facies Scc), sigmoidal cross-stratification (Facies Ssg), tangential cross-stratification (Facies Stg), trough cross-stratification (Facies St) and even-parallel stratification (Facies Sh) or are homogenized by bioturbation (Facies Sb). Additionally, wavy to flaser tidal rhythmites (Facies Hwf) and massive mud (Facies Mm) were observed. The Facies Ssg, Stg and Sp are interpreted as tidal bundle (*cf.* Boersma 1969) (Figs. 4C to 4F). Sand and mud intercalations with wavy bedding grading vertically into flaser bedding are interpreted as tidal rhythmites (Figs. 4G and 4H). Cross lamination is rare and generally the lenses are internally homogeneous. Some portions of the sandy facies are heavily bioturbated with no primary structures preserved (Facies Sb; Fig. 4I). Herringbone cross-stratification with mud drapes occurs locally and record flood-ebb tidal currents.

Tide-influenced meandering stream channel (FA2)

This facies assocation is characterized mainly by tabular geometry with rare and isolated channels interbedded with tidal deposits of FA1 (Figs. 5A to 5C). The very coarse-grained sands and gravel deposits of FA2 onlap basement rocks along an angular erosive

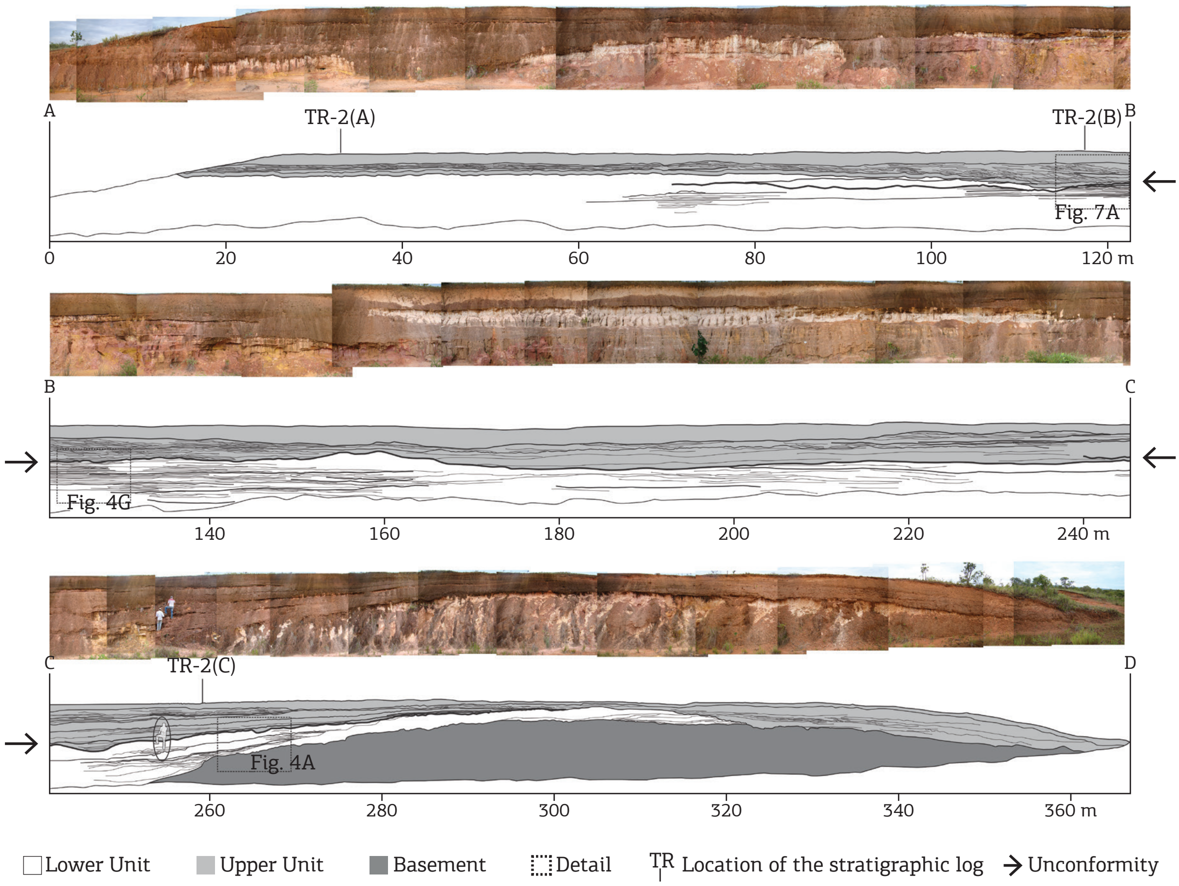

Figure 3. Photomosaic of TR2 in the Itaubal Formation exposed along BR-156 highway, near the town of Tartarugalzinho (Amapá State). The main characteristic of the Lower Unit is its tabular beds extending laterally over hundreds of meters, covered by mud drapes. The base of the Upper Unit is an undulating erosional unconformity.

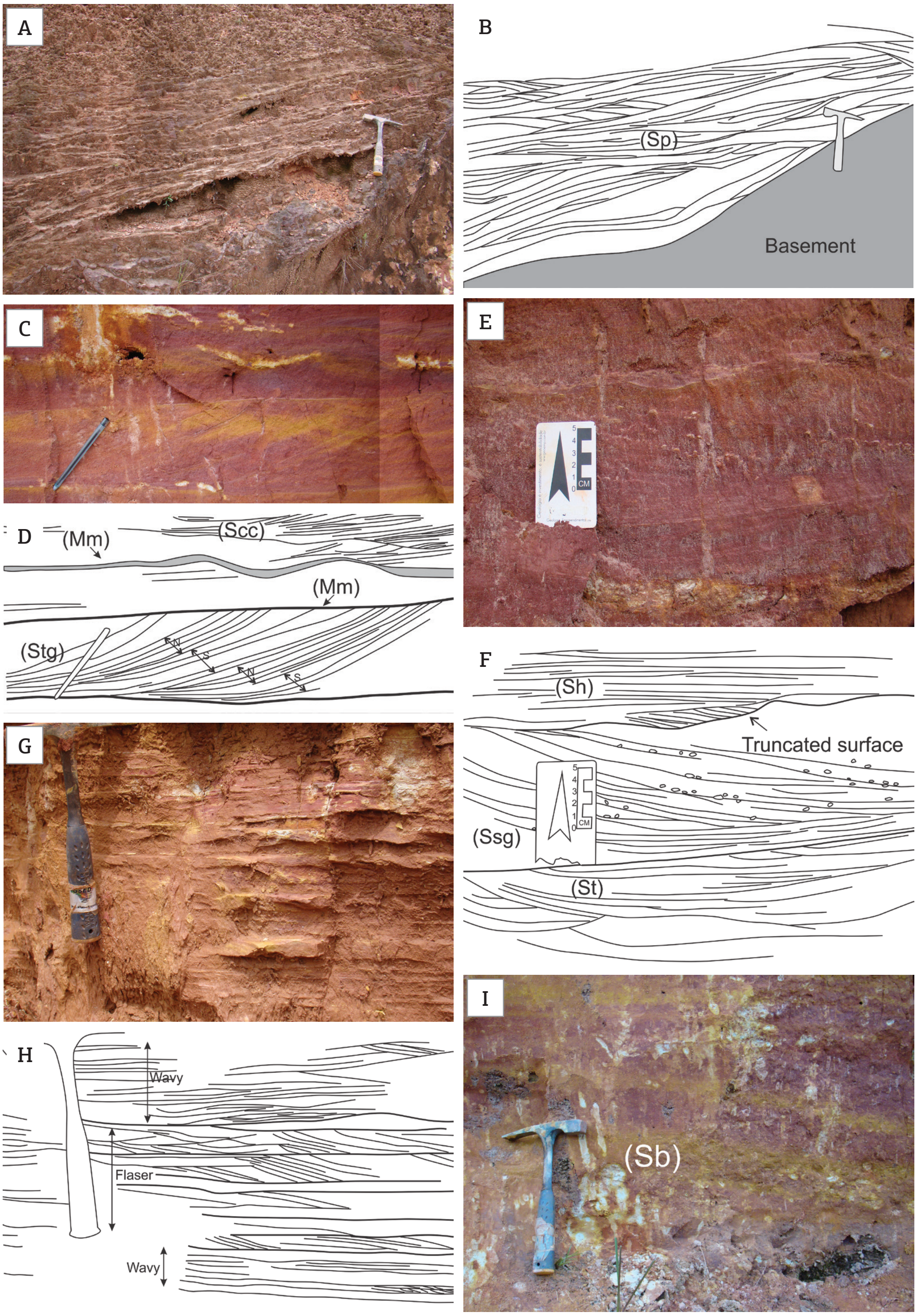

Sp: sand with tabular cross-stratification; Mm: massive mud; Scc: sand with climbing ripple cross-lamination; Stg: sand with tangential cross-stratification; Sh: sand with even parallel stratification; Ssg: sand with sigmoidal cross-stratification; St: sands with trough cross-stratification; Sb: bioturbated sand.

Figure 4. Field photographs and interpreted sketches of subtidal flat (FA1) deposits. (A and B) Sand and mud deposits onlapping the weathered basement. (C and D) facies Stg with tidal bundle made of spring-tide (S) and neap-tide (N) lamina sets. The bedform of the cross-bedding sets is preserved by mud layer (facies Mm). (E and F) the set of facies St is truncated by facies Ssg and Sh, with the same dip direction of the beds. Mud clast occurs in foreset of facies Ssg. (G and H) wavy bedding grading vertically into flaser bedding (facies Hwf). (I) bioturbated sand (facies Sb).

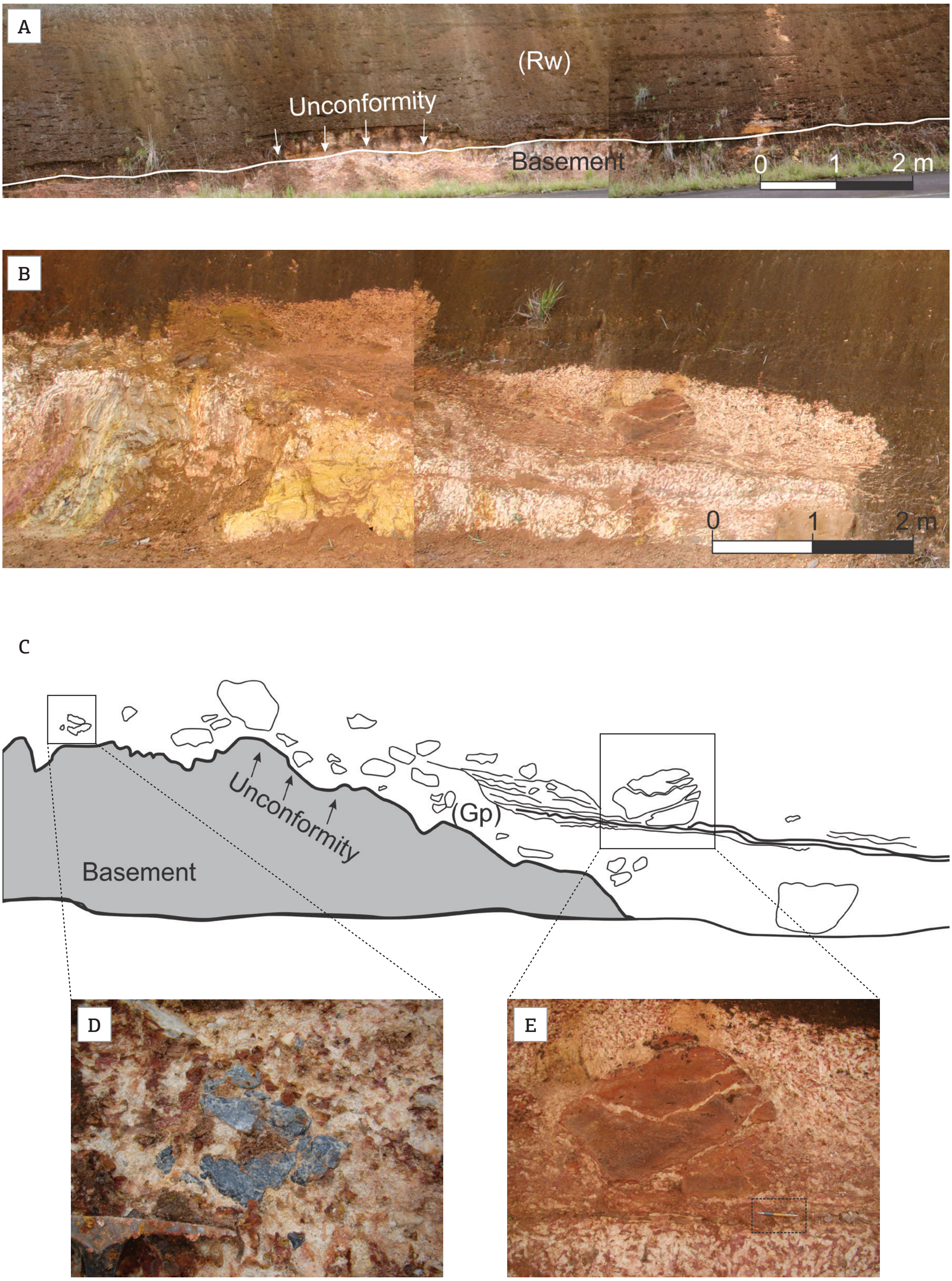

Rw: wavy-bedded rhythmites; Gp: Gravel with incipient even-parallel stratification

Figure 5. Geometry and contacts of the FA 2: tide-influenced meandering stream channel. (A) Onlap of facies Rw over basement. (B and C) angular erosive and channelized contact of the facies Gp with basement rocks. (D) gravels (10 cm) from facies Gp. (E) sandstone boulders of Facies Gp (80 cm).

contact (Tab. 2). Gravel with incipient even-parallel stratification contains pebbles and boulders of iron oxide/hydroxide cemented sandstones and volcanic rocks (Facies Gp) (Figs. 5D and 5E). Medium- to coarse-grained sand with trough cross-stratification (Facies St), medium-grained sand with tangential cross-stratification (Facies Stg), and wavy-bedded rhythmites (Facies Rw) are interbedded with Facies Gp. Inclined heterolithic cross-bedded sand and mud (Facies SMi) eventually marked by quartz pebbly lag and massive to laminated mud (Facies Mml) are commonly found in this association (Figs. 6A to 6D).

Floodplain (FA3)

This facies association comprise the upper portion of the Lower Unit and fill an erosional surface with an irregular relief developed on FA1 and FA2 (Figs. 3 and 7). This association has a maximum thickness of about 1 m and is laterally continuous over hundreds of meters. FA3 is organized in small-scale fining-upward cycles, composed of gravel deposits of intraformational mud clast (Facies Gi) and massive to laminated muds (Facies Mml) (Tab. 2). Mud deposits are generally mottled, showing red and white colors.

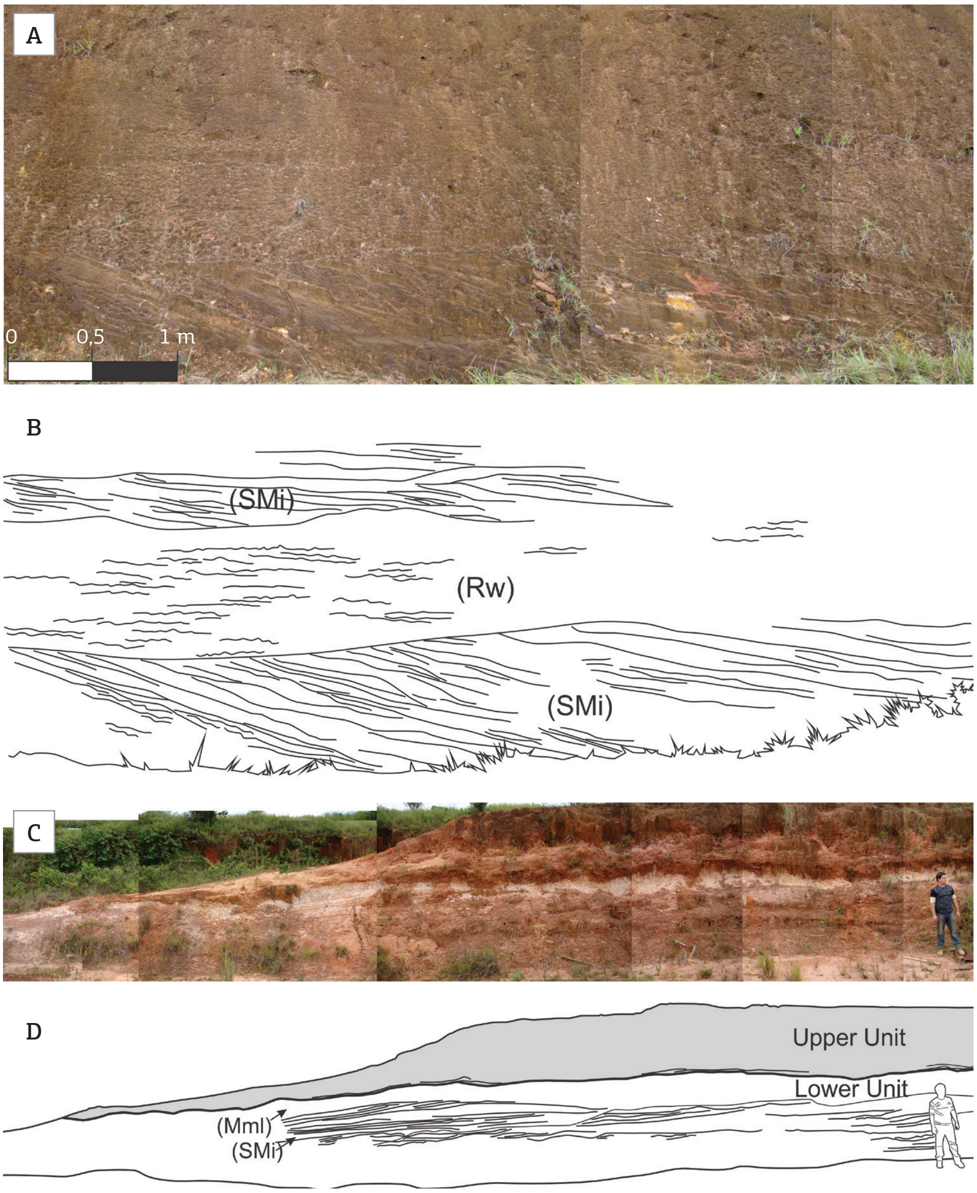

SMi: hetherolitic cross-bedding sets with alternating sand and mud laminae; Rw: wavy-bedded rhythmites; Mml: massive to laminated mud.

Figure 6. General appearance of Facies SMi. (A and B) Facies SMi interbedded with facies Rw. (C and D) facies SMi interbedded with facies Mml.

Upper unit

This 4-m-thick unit consists of brownish to whitish gravels, medium-to coarse-grained sand and mud and overlies an erosional unconformity (Fig. 2). The sandy deposits are characterized by tabular and rarely undulated beds, laterally continuous for hundreds of meters (Fig. 3). A bed of ferruginized sand at the base of this unit marks the contact with the Lower Unit. Cross bedding in the Upper Unit shows paleocurrent direction preferentially to NE. White sands are found along the studied area and are related to pedogenetic horizons or spodosols. The ferruginous soils are in part removed and fragmented, forming stone lines and stone layers on hillsides.

The Upper Unit is composed of six sedimentary facies grouped into the facies association FA4 and interpreted as braided stream channel deposits (Tab. 2). FA4 is characterized by ferruginous reddish lithified soil in the upper part (Figs. 7A and 7B). FA4 lies on an erosive contact with FA3 and locally forms channelized geometry. The braided stream channel deposits consist of moderately- to poorly-sorted and mostly medium- to coarse-grained sand with trough (Facies St), tabular (Facies Sp) and sigmoidal cross-stratifications (Facies Ssg) (Tab. 2). Massive mud deposits (Facies Mm) are common and are locally covered with Facies Ssg. Facies St is predominant in this association and generally exhibits gravelly lags composed of mud clasts and wood fragments, fossilized by iron oxide-hydroxides. Massive sandy beds with rare iron oxide concretions overlie quartzite and weathered volcanic basement rocks.

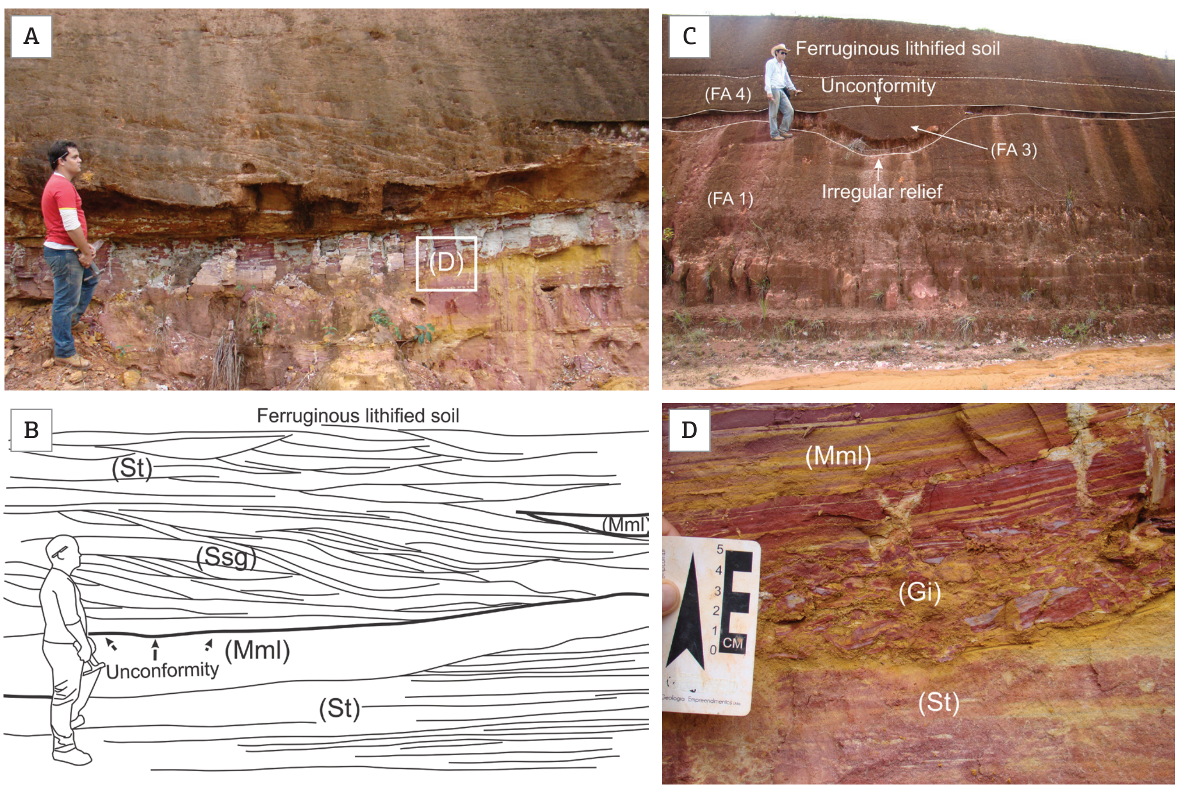

St: sands with trough cross-stratification; Ssg: sand with sigmoidal cross-stratification; Mml: massive to laminated mud; Gi: intraformational massive mud clast.

Figure 7. General appearance of the contact between Lower Unit and the Upper Unit. (A and B) Contact marked by an irregular relief filled by facies Mml, FA3 and FA4 interbedded with facies Ssg. (C) FA4 overlying FA3. (D) basal part of the FA3 marked by facies Gi reworking facies St of the Lower Unit.

DISCUSSION

Paleoenvironment evolution of the Itaubal Formation

The Itaubal Formation, which unconformably overlies a weathered Precambrian basement, consists of two progradational units, the Lower and Upper Units, separated by an unconformity, related to a sea-level fall. The presence of the Pleistocene Itaubal Formation just above the underlying strong weathering basement rocks suggests the absence of the Barreiras Formation in the ACP, and probably western border of the Marajó Graben being an uplifted area during the Miocene-Pliocene.

After the drowning of the putatively incised valleys, fine-grained deposits form an extensive tidal flat system in the ACP (Lower Unit), in highstand conditions (Fig. 8 and HSST 1 in Fig. 9 — stages 1 and 2). The Lower Unit represents tide-influenced deposits of the outer portion of the ACP between 120,600 (± 12,000) and 70,850 (± 6,700) years BP (Fig. 9 — stage 2). This event is correlated with the Last Interglacial and Marine Isotope Stage 5 and 4/5 (Lisiecki and Raymo 2005). Subaqueous dunes were the main bedforms in the tidal flat induced by tidal currents, alternating with slack water conditions (*e.g.* Visser 1980; Tessier 1993; Dalrymple and Choi 2007). Tide-influenced meandering fluvial channels were incised in the tidal flat and partially on the weathered basement. Point bars were deposited under moderate to lower energy flows in the concave up margin of channels (*e.g.* Thomas *et al.* 1987). Erosion of cut bank was accompanied of gravitational failures and generated intraformational deposits.

The event of falling-stage (FSST 1) promoted a renewal of fluvial incision between 69,150 (± 7,200) and 58,150 (± 6,800) years BP with the establishment of a high-energy braided stream environment, with ephemeral floodplains, prograding over tide deposits of the Lower Unit (Fig. 9 — stage 3). The lowstand conditions (LSST 2) remained until 23,500 (± 3,000) years BP, coinciding with the Last Glacial Maximum of the Wisconsin (Fig. 9 — stage 4) (Maslin and Burns 2000; Maslin *et al.* 2006; Miller *et al.* 2005). The Upper Unit is also correlated with Marine Isotope Stage 4, 3 and 2/3.

During the Last Glacial Maximum, the Itaubal Formation was entirely exposed, undergoing ferruginization and reworking. As a result, it was partially eroded and its remnants form currently residual terraces discontinuously distributed along the coast (Fig. 9 — stage 4). After this period, Holocene sands and muds from the Amazon River were deposited, forming the modern tidal flats of the ACP (Fig. 9 — stage 6; Guimarães *et al.* 2012, 2013b).

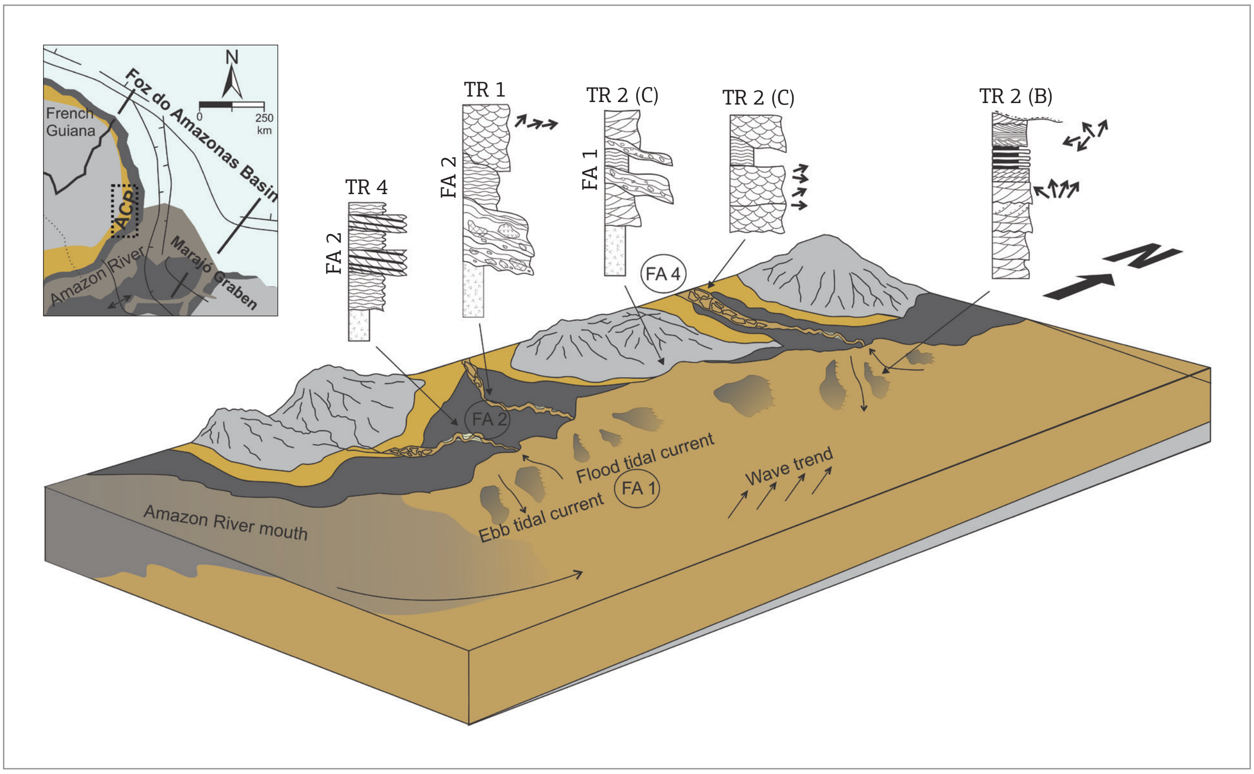

Figure 8. Depositional model of the Itaubal Formation.

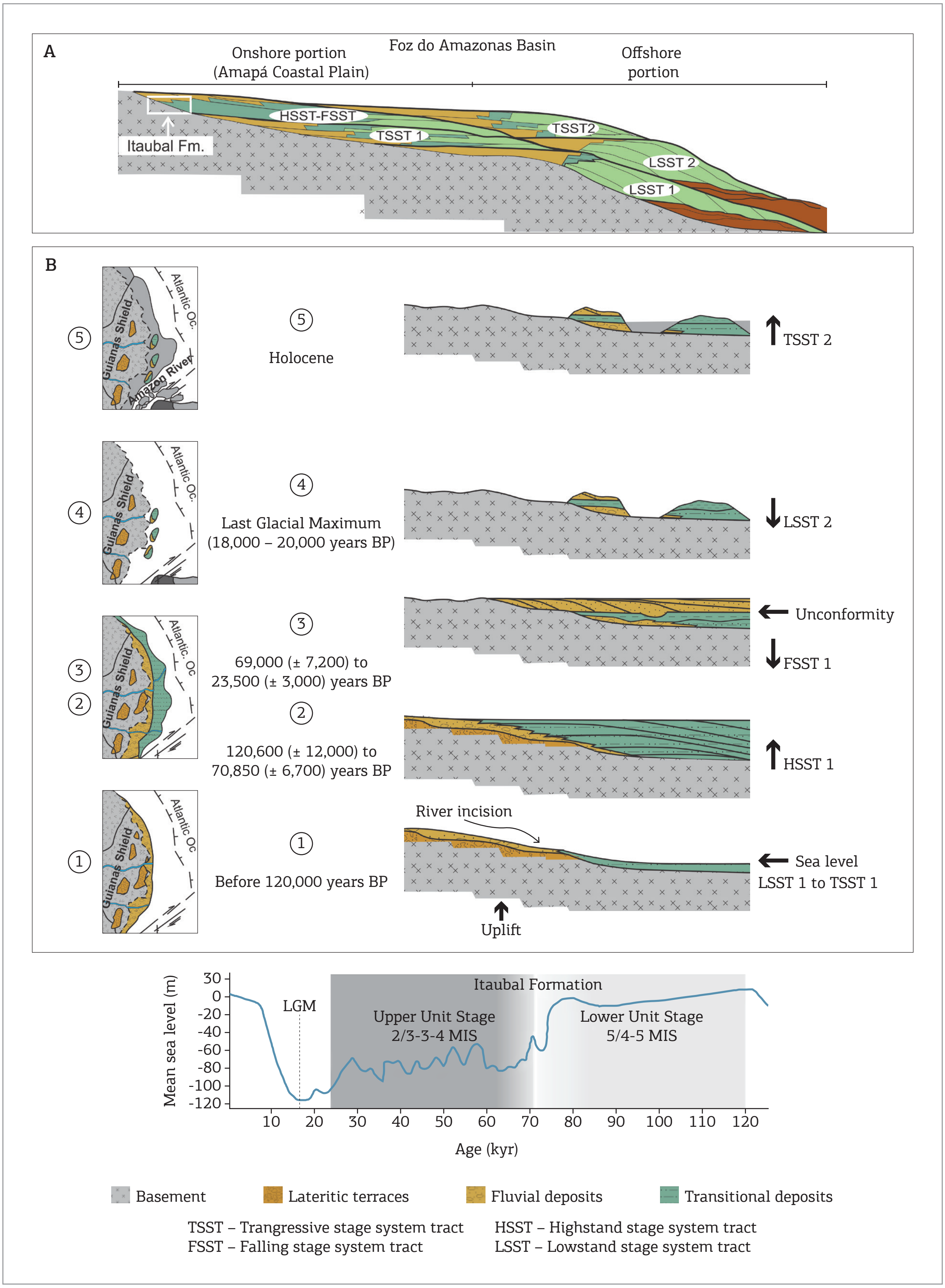

Figure 9. (A) Proposal for the system tract of the Foz do Amazonas Basin. The Itaubal Formation occurs in onshore portion. (B) Paleoenvironmental evolution and sea-level changes during the Itaubal Formation times and relation with sea-level curve from Maslin *et al.* (2006).

Correlation with Pleistocene units of northern South America

The evolution of the ACP is comparable with the Suriname Coastal Plain (SCP) (Fig. 10), located 200 km to the north of studied area. The Suriname Coast Plain has been traditionally being subdivided into two geomorphological domains: the older domain was developed mainly in Pleistocene deposits (Coropina Formation) and the younger domain under Holocene sediments (Mara and Coronie Formation) (Veen 1970; Wong 1992; Wong *et al*. 2009).

The sedimentary history of the Pleistocene Coropina Formation was influenced by global sea-level changes recorded in the Para and Lelydorp members. Braided stream deposits of the Para Member onlapped the bauxitic hardcaps, upper part of the Paleocene-Eocene Onverdacht Formation, called "Bauxite Hiatus" (Wong 1992; Wong *et al*. 2009). The development of this unconformity was related to a long period of non-deposition, during Late Eocene to Oligocene (Fig. 10). The meandering channel, chenier and lagoon deposits of the Lelydorp Member overlap weathered upper part of the Para Member and represent transgressive to highstand phase conditions (Veen 1970; Wong 1992; Wong *et al*. 2009). The Coropina Formation was entirely exposed due to sea-level fall, submitted to strongly weathering process and reworked by fluvial incision. Afterwards, a transgressive event occurred during the Holocene concomitant with deposition of the Coronie and Mara Formations (Brinkman and Pons 1968; Wong 1992; Wong *et al*. 2009).

The fluvial incision of the Para Member probably correlates with stage 1 (Fig. 9 — stage 1) in lowstand to transgressive conditions (LSST 1-TSST 1), while the upper portion of the Lelydorp Member, formed during transgressive to highstand conditions (HSST 1), may be related to the Lower Unit of the Itaubal Formation (Fig. 9 — stage 2).

The studied deposits are also correlated partially with the Pós-Barreiras sediments of the Marajó Graben system that overlies the Pliocene-Pleistocene lateritic paleosol (Góes 1981; Rossetti 2004) (Fig. 1). In contrast, Pleistocene deposits in the SCP overlie bauxitic surfaces formed during the Miocene-Pliocene and Eocene-Oligocene (Wong 1992; Wong *et al.* 2009). The Pós-Barreiras sediments initiated as fluvial deposits filling incised paleovalleys during a lowstand, probably correlates with stage 1 (Fig. 9 — stage 1), occurred before 120,000 years BP (Tatumi *et al.* 2008; Rosseti and Valeriano 2007).

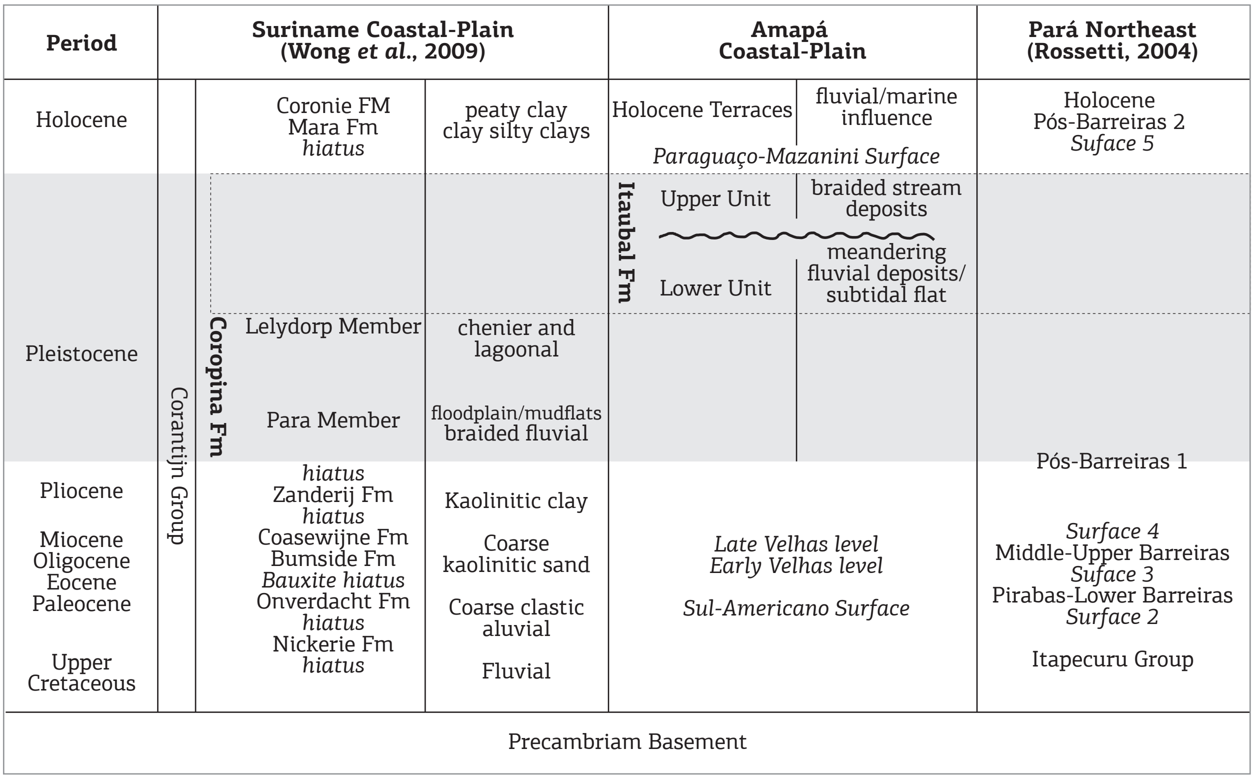

Figure 10. Chart showing the time equivalence of the Pleistocene units of northern South America (Bardossy & Aleva 1990; Rossetti 2004; Wong *et al*. 2009; Guimarães *et al*. 2012).

Around the 120,000 years BP, transgressive to highstand channel infill is found for the Lower Unit of the Itaubal Formation in the ACP and the upper portion of the Coropina Formation in the SCP.

CONCLUSION

Detailed facies and stratigraphic analyses in combination with high-resolution OSL data (single and multiple aliquot regeneration) from Pleistocene deposits, previously related to the Miocene Barreiras Formation, confirmed their Late Pleistocene age. Additionally, we name here these Pleistocene deposits "Itaubal Formation". This formation, exposed in the Amapá Coastal Plain, onshore portion of the Foz do Amazonas Basin, northeastern South America, unconformably overlies the weathered Precambrian basement. The formation was partially eroded and the current morphological configurations are residual terraces discontinuously exposed along the Amapá coast. Afterwards, Holocene tidal deposits partially covered the Itaubal deposits influenced by the fluvial processes related to the Amazon River discharges.

The Itaubal Formation was subdivided into two progradational units, separated by an erosional unconformity. The Lower Unit consists of subtidal and tide-influenced meandering stream and floodplain deposits distributed in the outer portion of the ACP. It reflects a highstand (stage phase) condition occurred between 120,600 (± 12,000) and 70,850 (± 6,700) years BP. This Lower Unit can be correlated with the upper portion of the Coropina Formation in the Suriname coastal plain and part of the Pós-Barreiras sediments of the Marajó Graben system. The Upper Unit was interpreted as braided stream deposits related to a base-level fall and falling-stage conditions, with yielded ages of 69,150 (± 7,200) and 58,150 (± 6,800). Lowstand conditions remained until 23,500 (± 3,000) years BP, during the Last Glacial Maximum, when the Itaubal Formation was exposed and submitted to ferruginization processes, which led to confusion with the iron-rich Miocene Barreiras deposits.

The absence of the Barreiras Formation in the ACP and the intensely weathered Precambrian basement rocks suggest the western border of the Marajó Graben being an uplifted area during Miocene-Pliocene that, as a geographic barrier, restricted the Miocene deposition in the Bragantina Plataform, northern State of Pará and Suriname Coastal Plain.

ACKNOWLEDGMENTS

This research received funds from Financiadora de Estudos e Projetos (FINEP)/Conselho Nacional de Desenvolvimento Científico e Tecnológico (CNPq)/Petróleo Brasileiro S.A. (PETROBRAS)/Fundo Nacional de Desenvolvimento Científico e Tecnológico (FNDCT) (2654.09-FINEP) for field trips and OSL dating. The first and second authors hold a CNPq scholarship. We thank Odete Fátima Machado da Silveira (*in memorian*) for discussions and comments relative to the geology of the State of Amapá. We are grateful to Eduardo Souza for their initial discussions about the presence of the Pleistocene deposits in the ACP, which motivated the continuity of this research. We also thank the useful suggestions made by the anonymous reviewer.

REFERENCES

Bardossy G. & Aleva G.J.J. 1990. *Lateritic bauxites*. Amsterdam, Elsevier, 624 p.

Boersma J.R. 1969. Internal structures of some tidal megaripples on a shoal in the Westerschelde estuary, the Netherlands. *Geologie en Mijnbouw*, **48**:409-414.

Boye M. & Cruys H. 1961. New data of the coastal sedimentary formations in French Guiana. *In*: 5º Inter-Guiana Geology Conference. Geological Survey Department, Georgetown, Guyana, *Proceedings*, p. 145-168.

Brandão J.A.S.L. & Feijó F.J. 1994. Bacia da Foz do Amazonas. *Boletim de Geociências da Petrobras*, **8**:91-94.

Brinkman R. & Pons L.J. 1968. A pedo-geomorphological classification and map of the Holocene sediments in the coastal plain of the three Guianas. v. 4. Wageningen, Soil Survey Institute, 41 p.

CPRM - Serviço Geológico do Brasil. 2004. Carta geológica do Brasil 1:1.000.*000*. Folha NA.22- Macapá. CD-ROM.

Dalrymple R.W. & Choi K. 2007. Morphologic and facies trends through the fluvial-marine transition in tide-dominated systems: a schematic framework for environmental and sequence-stratigraphic interpretation. *Earth-Science Reviews*, **81**(3):135-174.

Figueiredo J., Hoorn C., van der Ven P., Soares E. 2009. Late Miocene onset of the Amazon River and the Amazon deep-sea fan: evidence from the Foz do Amazonas Basin. *Geology*, **37**(7):619-622.

Folk R.L. 1974. *Petrology of sedimentary rocks*. Austin, Hemphill, 184 p.

Galvão M.V.G. 1991. *Evolução termodinâmica da Bacia do Marajó, Estado do Pará, Brasil*. MS Dissertation, Departamento de Geologia, Universidade Federal de Ouro Preto, Ouro Preto, 193 p.

Garzione C.N., Hoke G.D., Libarkin J.C., Withers S., Mac Fadden B., Eiler J., Ghosh P., Mulch A. 2008. Rise of the Andes. *Science*, **320**:1304-1307.

Góes A.M. 1981. *Estudo sedimentológico dos sedimentos Barreiras, Ipixuna e Itapecuru, no nordeste do Estado do Pará e noroeste do Maranhão*. MS Dissertation, Instituto de Geociências, Universidade Federal do Pará, Belém, 55 p.

Grossmann G.S. 2002. *Processamento e interpretação de dados sísmicos de Parasoud no delta submarino do Amazonas*. MS Dissertation, Departamento de Geologia, Universidade Federal Fluminense, Niterói, 78 p.

Guimarães J.T.F., Cohen M.C.L., Franca M.C., Pessenda L.C.R., Behling H. 2013a. Morphological and vegetation changes on tidal flats of the Amazon Coast during the last 5000 cal. yr BP. *The Holocene*, **23**(4):528-543.

Guimarães J.T.F., Cohen M.C.L., França M.C., Pessenda L.C.R., Souza E.J., Nogueira A.C.R., Alves R. 2013b. Recent effects of tidal and hydro-meteorological changes on coastal plains near the mouth of the Amazon River. *Earth Surface Processes and Landforms*, **38**:1535-1549.

Guimarães J.T.F., Cohen M.C.L., Pessenda L.C.R., Franca M.C., Smith C.B., Nogueira A.C.R. 2012. Mid- and late-Holocene sedimentary process and palaeovegetation changes near the mouth of the Amazon River. *The Holocene*, **22**(3):359-370.

Haq B.U., Handenbol J., Vail P.R. 1988. Mesozoic and Cenozoic chonostratigraphy and cycles of sea-level change. *In*: Wilgus C.K., Hastings B.S., Kendall C.G.ST.C., Posamentier H.W., Ross C.A., Van Wagoner J.C. (eds.). *Sea-level changes – an integrated approach*. Special Publication, v. 42. Tulsa, Society of Economic Paleontologists and Mineralogists, p. 71-108.

IBGE - Instituto Brasileiro de Geografia e Estatística. 2003. Base cartográfica integrada digital do Brasil ao milionésimo: versão 1.0 para ArcGis Desktop-ArcView. Rio de Janeiro: IBGE, 1 CD-ROM.

Krook L. 1979. *Sediment petrographical studies of the Surinam coastal area*. PhD Thesis, Free University, Amsterdam, 154 p.

Lima M.I.C., Bezerra P.E.L., Araújo H.J.T. 1991. Sistematização da geologia do estado do Amapá. *In*: Simpósio de Geologia da Amazônia. Belém, SBG-Núcleo Norte, v. 3, *Anais*, p. 322-335.

Lima M.I.C., Montalvão R.M.G., Issler R.S., Oliveira A.S., Basei M.A.S., Araújo J.F.V., Silva G.G. 1974. Geologia Folha NA/22 (Macapá). Levantamento de Recursos Naturais, v. 6. Rio de Janeiro, Projeto RADAM, Departamento Nacional de Produção Mineral, p. 1-120.

Lisiecki L.E. & Raymo M.E. 2005. A Pliocene-Pleistocene stack of 57 globally distributed benthic $\delta^{18}O$ records. *Paleoceanography*, **20**(1):PA1003.

Lopez M. 2001. Architecture and depositional pattern of the Quaternary deep-sea fan of the Amazon. *Marine and Petroleum Geology*, **18**(4):479-486.

Maslin M.A. & Burns S.J. 2000. Reconstruction of the Amazon Basin effective moisture availability over the past 14,000 years. *Science*, **290**(5500):2285-2287.

Maslin M.A., Knutz P.C., Ramsay T. 2006. Millenial-scale sea-level control on avulsion events on the Amazon Fan. *Quaternary Science Reviews*, **25**(23-24):3338-3345.

Mendes A.C. 1994. *Estudo sedimentológico e estratigráfico dos sedimentos holocênicos da costa do Amapá - Setor entre a Ilha de Maracá e o Cabo Orange*. MS Dissertation, Instituto de Geociências, Universidade Federal do Pará, Belém, 274 p.

Miall A.D. 1991. Hierarchies of architectural units in terrigenous clastic rocks and their relationship to sedimentation rate. *In*: Miall A.D. & Tyler N. (eds.). *The three dimensional facies architecture of terrigenous clastic sediments and its implications for hidrocarbon discovery and recovery*. Tulsa, Society for Sedimentary Geology/SEPM, p. 6-12.

Miall A.D. 1994. Reconstructing fluvial macroform architecture from two-dimensional outcrops: examples from the Castlegate Sandstone, Book Cliffs, Utah. *Journal of Sedimentary Research*, **64**(2B):146-158.

Miller K.G., Fairbanks R.G., Mountain G.S. 1987. Tertiary oxygen isotope synthesis, sea-level history, and continental margin erosion. *Paleoceanography*, **2**(1):1-19.

Miller K.G., Kominz M.A., Browning J.V., Wright J.D., Mountain G.S., Katz M.E., Sugarman P.J., Cramer B.S., Christie-Blick N., Pekar S.F. 2005. The Phanerozoic record of global sea-level change. *Science*, **310**(5752):1293-1298.

Murray A.S. & Wintle A.G. 2000. Luminescence dating of quartz using an improved single-aliquot regenerative dose protocol. *Radiation Measurements*, **32**(1):57-73.

Rodarte J.B.M. & Brandão J.A.S.L. 1988. Arcabouço estrutural, estratigrafia e perspectivas exploratórias da área de Cassiporé, porção noroeste da Bacia da Foz do Amazonas. Rio de Janeiro, PETROBRAS.

Roeleveld W. & Van Loon A.J. 1979. The Holocene development of the Young Coastal Plain of Suriname. *Geologie en Mijnbouw*, **58**:21-28.

Rossetti D.F. 2004. Paleosurfaces from northeastern Amazonia as a key for reconstructing paleolandscapes and understanding weathering products. *Sedimentary Geology*, **169**(3-4):151-174.

Rossetti D.F., Rocca R.R., Tatumi S.H. 2013. Datação de sedimentos pós-barreiras, município de Alcântara, litoral maranhense. *Boletim do Museu Paraense Emílio Goeldi (Ciências Naturais)*, **8**:11-25.

Rossetti D.F., Trukenbrodt W., Góes A.M. 1989. Estudo paleoambiental e estratigráfico dos sedimentos Barreiras e Pós-Barreiras na região Bragantina, nordeste do Pará. *Boletim do Museu Paraense Emílio Goeldi (Série Ciências da Terra)*, **1**:25-74.

Rossetti D.F. & Valeriano M.M. 2007. Evolution of the lowest Amazon Basin modeled from the integration of geological and SRTM topographic data. *Catena*, **70**(2):253-265.

Santos V.F. 2006. *Ambientes costeiros amazônicos*: avaliação de modificações por sensoriamento remoto. PhD Thesis, Instituto de Geociências, Universidade Federal Fluminense, Niterói, 306 p.

Silveira O.F.M. 1998. *A Planície costeira do Amapá:* dinâmica de ambiente costeiro influenciada por grandes fontes fluviais quaternárias. PhD Thesis, Instituto de Geociências, Universidade Federal do Pará, Belém, 215 p.

Soares Júnior A.V., Costa J.B.S., Hasui Y. 2008. Evolução da margem atlântica equatorial do Brasil: três fases distensivas. *Geociências*, **27**(4):427-437.

Souza E.J. 2010. *Geologia da região costeira do Amapá com ênfase na estratigrafia, morfotectônica e geomorfologia*. Monografia de Conclusão de Curso, Faculdade de Geologia, Universidade Federal do Pará, Belém, 118 p.

Tatumi S.H., Silva L.P., Pires E.L., Rossetti D.F., Góes A.M. 2008. Datação de sedimentos pós-barreiras no norte do Brasil: implicações paleogeográficas. *Revista Brasileira de Geociências*, **38**(3):514-524.

Tessier B. 1993. Upper intertidal rhythmites in the Mont-Saint-Michel Bay (NW France): perspectives for paleoreconstruction. *Marine Geology*, **110**(3-4):355-367.

Thomas R.G., Smith D.G., Wood J.M., Visser J., Calverley-Range E.A., Koster E.H. 1987. Inclined heterolithic stratification – terminology, description, interpretation and significance. *Sedimentary Geology*, **53**(1-2):123-179.

Uba C.E., Strecker M., Schmitt A.K. 2007. Increased sediment accumulation rates and climatic forcing in the Central Andes during the late Miocene. *Geology*, **35**(11):979-982.

Veen A.W.L. 1970. *On geogenesis and pedogenesis in the Old Coastal Plain of Surinam (South-America)*, v. 14. Amsterdam, Fysisch-Geografisch en Bodemkundig Laboratorium, 176 p.

Visser M.J. 1980. Neap-spring cycles reflected in Holocene subtidal large-scale bedform deposits: a preliminary note. *Geology*, **8**(11):543-546.

Walker R.G. 1992. Facies, facies models and modern stratigraphic concepts. *In*: Walker R.G. & James N.P. (eds.). *Facies models* - response to sea-level change. Ontario, Geological Association of Canada, p. 1-14.

Wong T.E. 1992. Quaternary stratigraphy of Suriname. *In*: Prost M.T. & Charron C. (eds.). Evolution des littoraux de Guyane et de la zone caraïbe méridionale pendant le Quaternaire. *In*: Symposium PICG 274/Orstom, Cayenne (Guyane), 9-14 November 1990. Orstom, Paris, p. 559-578.

Wong T.E., de Kramer R., de Boer P.L., Langereis C., Sew-A-Tjon J. 2009. The influence of sea-level changes on tropical coastal lowlands; the Pleistocene Coropina Formation, Suriname. *Sedimentary Geology*, **216**(3-4):127-137.

Arquivo digital disponível on-line no site www.sbgeo.org.br